

# Multi-Task Classification Hypothesis Space with Improved Generalization Bounds

Cong Li, Michael Georgiopoulos and Georgios C. Anagnostopoulos

CL, MG: EE & CS Dept., University of Central Florida; GCA: ECE Dept., Florida Institute of Technology

congli@eecs.ucf.edu, michaelg@ucf.edu and georgio@fit.edu

## Abstract

This paper presents a RKHS, in general, of vector-valued functions intended to be used as hypothesis space for multi-task classification. It extends similar hypothesis spaces that have previously considered in the literature. Assuming this space, an improved Empirical Rademacher Complexity-based generalization bound is derived. The analysis is itself extended to an MKL setting. The connection between the proposed hypothesis space and a Group-Lasso type regularizer is discussed. Finally, experimental results, with some SVM-based Multi-Task Learning problems, underline the quality of the derived bounds and validate the paper's analysis.

**Keywords:** Multi-task Learning, Kernel Methods, Generalization Bound, Support Vector Machines

## 1 Introduction

Multi-Task Learning (MTL) has been an active research field for over a decade [4]. The fundamental philosophy of MTL is to simultaneously train several related tasks with shared information, so that the hope is to improve the generalization performance of each task by the assistance of other tasks. More formally, in a typical MTL setting with  $T$  tasks, we want to choose  $T$  functions  $f = (f_1, \dots, f_T)$  from a Hypothesis Space (HS)  $\mathcal{F} = \{\mathbf{x} \mapsto [f_1(\mathbf{x}), \dots, f_T(\mathbf{x})]'\}$ , where  $\mathbf{x}$  is an instance of some input set  $\mathcal{X}$ , such that the performance of each task is optimized based on a problem-specific criterion. Here  $[f_1(\mathbf{x}), \dots, f_T(\mathbf{x})]'$  denotes the transposition of row vector  $[f_1(\mathbf{x}), \dots, f_T(\mathbf{x})]$ . MTL has been successfully applied in feature selection [2, 8, 10], regression [19, 16], metric learning [28][23], and kernel-based MTL [7, 3, 24, 1] among other applications.

Despite the abundance of MTL applications, relevant generalization bounds have only been developed for special cases. A theoretically well-studied MTL framework is regularized linear MTL model, whose generalization bound is studied in [21, 13, 22]. In this framework, each function  $f_t$  is featured as a linear function with weight  $\mathbf{w}_t \in \mathcal{H}$ , such that  $\forall \mathbf{x} \in \mathcal{X} \subseteq \mathcal{H}, f_t(\mathbf{x}) = \langle \mathbf{w}_t, \mathbf{x} \rangle$ , where  $\mathcal{H}$  is a real Hilbert space equipped with inner product  $\langle \cdot, \cdot \rangle$ . Different regularizers can be employed to the weights  $\mathbf{w} = (\mathbf{w}_1, \dots, \mathbf{w}_T) \in \underbrace{\mathcal{H} \times \dots \times \mathcal{H}}_{T \text{ times}}$  to fulfill different requirements of the problem at hand. Formally, given  $\{\mathbf{x}_t^i, y_t^i\} \in \mathcal{X} \times \mathcal{Y}, i = 1, \dots, n_t, t = 1, \dots, T$ , where  $\mathcal{X}$  and  $\mathcal{Y}$  are the input and output space for each task, the framework can be written as

$$\min_{\mathbf{w}} R(\mathbf{w}) + \lambda \sum_{i,t} L(f_t(\mathbf{x}_t^i), y_t^i) \quad (1)$$

where  $R(\cdot)$  and  $L(\cdot, \cdot)$  are the regularizer and loss function respectively. Many MTL models fall into this framework. For example, [5] looks for group sparsity of  $\mathbf{w}$ , [29] discovers group structure of multiple tasks, and [8, 10] select features in a MTL context.

In the previous framework, tasks are implicitly related by regularizers on  $\mathbf{w}$ . On the other hand, another angle of considering information sharing amongst tasks is by pre-processing the data from all tasks by a common processor, and subsequently, a linear model is learned based on the processed data. One scenario of this learning framework is subspace learning, where data of each task are projected to a common subspace by an operator  $A$ , and then the  $\mathbf{w}_t$ 's are learned in that subspace. Such an approach is followed in [2, 14]. Another particularly straightforward and useful adaptation of this framework is kernel-based MTL. In this situation, the role of the operator  $A$  is assumed by the non-linear feature mapping  $\phi$  associated with the kernel function in use. In this case, all data are pre-processed by a *common* kernel function, which is pre-selected or learned during the training phase, while the  $\mathbf{w}_t$ 's are then learned in the corresponding Reproducing Kernel Hilbert Space (RKHS). One example of this technique is given in [26].

One previous work which discussed the generalization bound of this method in a classification context is [20]. Given a set  $\mathcal{A}$  of bounded self-adjoint linear operators on  $\mathcal{X}$  and  $T$  linear functions with weights  $\mathbf{w}_t$ 's, the HS is given as  $\mathcal{F} = \{\mathbf{x} \mapsto [\langle \mathbf{w}_1, A\mathbf{x} \rangle, \dots, \langle \mathbf{w}_T, A\mathbf{x} \rangle]' : \|\mathbf{w}_t\|^2 \leq R, A \in \mathcal{A}\}$ . Clearly, in this HS, data are pre-processed by the operator  $A$  to a common space, as a strategy of information sharing amongst tasks. By either cleverly choosing  $A$  beforehand or by learning  $A \in \mathcal{A}$ , it is expected that a tighter generalization bound can be attained compared to learning each task independently. It is straightforward to see that pre-selecting  $A$  beforehand is a special case of learning  $A \in \mathcal{A}$ , *i.e.*, pre-selecting  $A$  is equivalent to  $\mathcal{A} = \{A\}$ .

However, the limitations of  $\mathcal{F}$  are two-fold. First, in  $\mathcal{F}$ , all  $\mathbf{w}_t$ 's are equally constrained in a ball, whose radius  $R$  is determined prior to training. However, in practice, the HS that lets each task have its own radius for the corresponding norm-ball constraint may be more appropriate and may lead to a better generalization bound and performance.

The second limitation is that it cannot handle the models which learn a common kernel function for all tasks, *e.g.*, the Multi-Task Multiple Kernel Learning (MT-MKL) models. One way to incorporate such kernel learning models into  $\mathcal{F}$  is to let  $A$  be the feature mapping  $\phi : \mathcal{X} \mapsto \mathcal{H}_\phi$ , where  $\mathcal{H}_\phi$  is the output space of the feature mapping  $\phi$  and  $\phi$  corresponds to the common kernel function  $k$ . In other words, this setting defines  $\mathcal{F} = \{\mathbf{x} \mapsto [\langle \mathbf{w}_1, \phi(\mathbf{x}) \rangle, \dots, \langle \mathbf{w}_T, \phi(\mathbf{x}) \rangle]' : \|\mathbf{w}_t\|^2 \leq R, \phi \in \Omega(\phi)\}$ , where  $\Omega(\phi)$  is the set of feature mappings that  $\phi$  is learned from. Obviously, the HS that is considered in [20] does not cover this scenario, since it only allows the operator  $A$  to be linear operator, which is not the case when  $A = \phi$ . Yet another limitation reveals itself, when one considers the equivalent HS:  $\mathcal{F} = \{\mathbf{x} \mapsto [\langle \mathbf{w}_1, \mathbf{x} \rangle, \dots, \langle \mathbf{w}_T, \mathbf{x} \rangle]' : \|\mathbf{w}_t\|^2 \leq R, \mathbf{x} \in \mathcal{H}_\phi, \phi \in \Omega(\phi)\}$ , where, as mentioned above,  $\mathcal{H}_\phi$  is the output space of the feature mapping  $\phi$ . Obviously, the HS in [20] fails to cover this HS, due to the lack of the constraint  $\phi \in \Omega(\phi)$ , which indicates that the feature mapping  $\phi$  (hence, its corresponding kernel function) is learned during the training phase instead of being selected beforehand.

Therefore, in this paper, we generalize  $\mathcal{F}$ , particularly for kernel-based classification problems, by considering the common operator  $\phi$  (which is associated with a kernel function) for all tasks and by imposing norm-ball constraints on the  $\mathbf{w}_t$ 's with different radii that are learned during the training process, instead of being chosen prior to training. Specifically, we consider the HS

$$\mathcal{F}_s \triangleq \{\mathbf{x} \mapsto [\langle \mathbf{w}_1, \phi(\mathbf{x}) \rangle, \dots, \langle \mathbf{w}_T, \phi(\mathbf{x}) \rangle]' : \|\mathbf{w}_t\|^2 \leq \lambda_t^2 R, \boldsymbol{\lambda} \in \Omega_s(\boldsymbol{\lambda})\} \quad (2)$$

and

$$\mathcal{F}_{s,r} \triangleq \{\mathbf{x} \mapsto [\langle \mathbf{w}_1, \phi(\mathbf{x}) \rangle, \dots, \langle \mathbf{w}_T, \phi(\mathbf{x}) \rangle]' : \|\mathbf{w}_t\|^2 \leq \lambda_t^2 R, \boldsymbol{\lambda} \in \Omega_s(\boldsymbol{\lambda}), \phi \in \Omega_r(\phi)\} \quad (3)$$

where  $\Omega_s(\boldsymbol{\lambda}) \triangleq \{\boldsymbol{\lambda} \succeq \mathbf{0}, \|\boldsymbol{\lambda}\|_s \leq 1, s \geq 1\}$ , and  $\Omega_r(\phi) = \{\phi : \phi = (\sqrt{\theta_1}\phi_1, \dots, \sqrt{\theta_M}\phi_M), \boldsymbol{\theta} \succeq \mathbf{0}, \|\boldsymbol{\theta}\|_r \leq 1, r \geq 1\}$ ,  $\phi_m \in \mathcal{H}_m$ ,  $\phi \in \mathcal{H}_1 \times \dots \times \mathcal{H}_M$ . The objective of our paper is to derive and analyze the generalization bounds of these two HS. Specifically, the first HS,  $\mathcal{F}_s$ , has fixed feature mapping  $\phi$ , which is pre-selected, and the second HS,  $\mathcal{F}_{s,r}$ , learns the feature mapping via a Multiple Kernel Learning (MKL) approach. We refer readers to [18] and a survey paper [9] for details on MKL.

Obviously, by letting all  $\lambda_t$ 's equal 1,  $\mathcal{F}_s$  degrades to the equal-radius HS, which is a special case of  $\mathcal{F}_s$  when  $s \rightarrow +\infty$ , as we will show in the sequel. By considering the generalization bound of  $\mathcal{F}_s$  based on the Empirical Rademacher Complexity (ERC) [21], we first demonstrate that the ERC is monotonically increasing with  $s$ , which implies that the tightest bound is achieved, when  $s = 1$ . We then provide an upper bound for the ERC of  $\mathcal{F}_s$ , which also monotonically increases with respect to  $s$ . In the optimal case ( $s = 1$ ),

we achieve a generalization bound of order  $O(\frac{\sqrt{\log T}}{T})$ , which decreases relatively fast with increasing  $T$ . On the other hand, when  $s \rightarrow +\infty$ , the bound does not decrease with increasing  $T$ , thus, it is less preferred.

We then derive the generalization bound for the HS  $\mathcal{F}_{s,r}$ , which still features a bound of order  $O(\frac{\sqrt{\log T}}{T})$  when  $s = 1$ , as in the single-kernel setting. Additionally, if  $M$  kernel functions are involved, the bound is of order  $O(\sqrt{\log M})$ , which has been proved to be the best bound that can be obtained in single-task multi-kernel classification [6]. Therefore, the optimal order of the bound is also preserved in the MT-MKL case. Note that the proofs of all theoretical results are in the Appendix.

After investigating the generalization bounds, we experimentally show that our bound on the ERC matches the real ERC very well. Moreover, we propose a MTL model based on Support Vector Machines (SVMs) as an example of a classification framework that uses  $\mathcal{F}_s$  as its HS. It is further extended to an MT-MKL setting, whose HS becomes  $\mathcal{F}_{s,r}$ . Experimental results on multi-task classification problems show the effect of  $s$  on the generalization ability of our model. In most situations, the optimal results are indeed achieved, when  $s = 1$ , which matches our technical analysis. For some other results that are not optimal as expected, when  $s = 1$ , we provide a justification.

## 2 Fixed Feature Mapping

Let  $\{\mathbf{x}_t^i, y_t^i\} \in \mathcal{X} \times \{-1, 1\}$ ,  $i = 1, \dots, N$ ,  $t = 1, \dots, T$  be i.i.d. training samples from some joint distribution. Without loss of generality and on grounds of convenience, we will assume an equal number of training samples for each task. Let  $\mathcal{H}$  be a RKHS with reproducing kernel function  $k(\cdot, \cdot) : \mathcal{X} \times \mathcal{X} \mapsto \mathbb{R}$ , and associated feature mapping  $\phi : \mathcal{X} \mapsto \mathcal{H}$ . In what follows we give the theoretical analysis of our HS  $\mathcal{F}_s$ , when the feature mapping  $\phi$  is fixed.

### 2.1 Theoretical Results

Given  $T$  tasks, our objective is to learn  $T$  linear functionals  $f_t(\cdot) : \mathcal{H} \mapsto \mathbb{R}$ , such that  $f_t(\phi(\mathbf{x})) = \langle \mathbf{w}_t, \phi(\mathbf{x}) \rangle$ ,  $t = 1, \dots, T$ ,  $\mathbf{x} \in \mathcal{X}$ . Next, let  $\mathbf{f} \triangleq [f_1, \dots, f_T]'$ , and define the multi-task classification error as

$$er(f) \triangleq \frac{1}{T} \sum_{t=1}^T E\{\mathbf{1}_{(-\infty, 0]}(y_t f_t(\phi(\mathbf{x}_t)))\} \quad (4)$$

where  $\mathbf{1}_{(-\infty, 0]}(\cdot)$  is the characteristic function of  $(-\infty, 0]$  and referred to as the 0/1 loss function. The empirical error based on a surrogate loss function  $\bar{L} : \mathbb{R} \mapsto [0, 1]$ , which is a Lipschitz-continuous function that upper-bounds the 0/1 loss function, is defined as

$$\hat{er}(f) \triangleq \frac{1}{TN} \sum_{t,i=1}^{T,N} \bar{L}(y_t^i f_t(\phi(\mathbf{x}_t^i))) \quad (5)$$

For the constraints on the  $\mathbf{w}_t$ 's, instead of pre-defining a common radius  $R$  for all tasks as discussed in [20], we let  $\|\mathbf{w}_t\|^2 \leq \lambda_t^2 R$ , where  $\lambda_t$  is learned during the training phase. This motivates our consideration of  $\mathcal{F}_s$  as given in (2), which we repeat here:

$$\mathcal{F}_s \triangleq \{\mathbf{x} \mapsto [\langle \mathbf{w}_1, \phi(\mathbf{x}) \rangle, \dots, \langle \mathbf{w}_T, \phi(\mathbf{x}) \rangle] : \|\mathbf{w}_t\|^2 \leq \lambda_t^2 R, \boldsymbol{\lambda} \in \Omega_s(\boldsymbol{\lambda})\} \quad (6)$$

Note that the feature mapping  $\phi$  is determined before training. In order to derive the generalization bound for  $\mathcal{F}_s$ , we first provide the following lemma.

**Lemma 1.** *Let  $\mathcal{F}_s$  be as defined in Equation (6). Let  $\bar{L} : \mathbb{R} \mapsto [0, 1]$  be a Lipschitz-continuous loss function with Lipschitz constant  $\gamma$  and upper-bound the 0/1 loss function  $\mathbf{1}_{(-\infty, 0]}(\cdot)$ . Then, with probability  $1 - \delta$  we have*

$$er(f) \leq \hat{er}(f) + \frac{1}{\gamma} \hat{R}(\mathcal{F}_s) + \sqrt{\frac{9 \log \frac{2}{\delta}}{2TN}}, \quad \forall f \in \mathcal{F}_s \quad (7)$$

where  $\hat{R}(\mathcal{F}_s)$  is the ERC for MTL problems defined in [21]:

$$\hat{R}(\mathcal{F}_s) \triangleq E_\sigma \left\{ \sup_{\mathbf{f} \in \mathcal{F}_s} \frac{2}{TN} \sum_{t,i=1}^{TN} \sigma_t^i f_t(\phi(\mathbf{x}_t^i)) \right\} \quad (8)$$

where the  $\sigma_t^i$ 's are i.i.d. Rademacher-distributed (i.e., Bernoulli  $(\frac{1}{2})$ -distributed random variables with sample space  $\{-1, +1\}$ ).

This lemma can be simply proved by utilizing Theorem 16 and 17 in [20]. By using the same proving strategy, it is easy to show that (7) is valid for all HSs that are considered in this paper. Therefore, we will not explicitly state a specialization of it for each additional HS encountered in the sequel. In the next, we first define the following duality mapping for all  $a \in \mathbb{R}$ :

$$(\cdot)^* : a \mapsto a^* \triangleq \begin{cases} \frac{a}{a-1}, & \forall a \neq 1 \\ +\infty, & a = 1 \end{cases} \quad (9)$$

then we give the following results which show that  $\hat{R}(\mathcal{F}_s)$  is monotonically increasing with respect to  $s$ .

**Lemma 2.** Let  $\boldsymbol{\sigma}_t \triangleq [\sigma_t^1, \dots, \sigma_t^N]'$ ,  $u_t \triangleq \sqrt{\boldsymbol{\sigma}_t' \mathbf{K}_t \boldsymbol{\sigma}_t}$ , where  $\mathbf{K}_t$  is the kernel matrix that consists of elements  $k(\mathbf{x}_t^i, \mathbf{x}_t^j)$ ,  $t = 1, \dots, T$ ,  $\mathbf{u} \triangleq [u_1, \dots, u_T]'$ . Then  $\forall s \geq 1$

$$\hat{R}(\mathcal{F}_s) = \frac{2}{TN} \sqrt{R} E_\sigma \{ \|\mathbf{u}\|_{s^*} \} \quad (10)$$

Leveraging from Equation (10), one can show the following theorem.

**Theorem 1.**  $\hat{R}(\mathcal{F}_s)$  is monotonically increasing with respect to  $s$ .

Define  $\tilde{\mathcal{F}} \triangleq \{\mathbf{x} \mapsto [\langle \mathbf{w}_1, \phi(\mathbf{x}) \rangle, \dots, \langle \mathbf{w}_T, \phi(\mathbf{x}) \rangle] : \|\mathbf{w}_t\|^2 \leq R\}$ , which is the HS that is given in [20] under kernelized MTL setting, then  $\tilde{\mathcal{F}}$  is the HS with equal radius for each  $\|\mathbf{w}_t\|^2$ . Obviously, it is the special case of  $\mathcal{F}_s$  with all  $\lambda_t$ 's be set to 1. We have the following result:

**Theorem 2.**  $\hat{R}(\tilde{\mathcal{F}}) = \hat{R}(\mathcal{F}_{+\infty})$ .

The above results imply that the tightest generalization bound is obtained when  $s = 1$ , while, on the other hand, the bound of  $\mathcal{F}_{+\infty}$  that sets equal radii for all  $\mathbf{w}_t$ 's is the least preferred. It is clear that, to derive a generalization bound for  $\mathcal{F}_s$ , we need to compute, or, at least find an upper bound for  $\hat{R}(\mathcal{F}_s)$ . The following theorem addresses this requisite.

**Theorem 3.** Let  $\mathcal{F}_s$  be as defined in Equation (6), and let  $\rho \triangleq 2 \ln T$ . Assume that  $\forall \mathbf{x} \in \mathcal{X}$ ,  $k(\mathbf{x}, \mathbf{x}) = \langle \phi(\mathbf{x}), \phi(\mathbf{x}) \rangle \leq 1$ . Then the ERC can be bounded as follows:

$$\hat{R}(\mathcal{F}_s) \leq \frac{2}{T\sqrt{N}} \sqrt{\tau R T^{\frac{2}{s^*}}} \quad (11)$$

where  $\tau \triangleq (\max\{s, \rho^*\})^*$ .

## 2.2 Analysis

It is worth pointing out some observations regarding the result of Theorem 3.

- It is not difficult to see that the bound of the ERC in (11) is monotonically increasing in  $s$ , as is  $\hat{R}(\mathcal{F}_s)$ .
- As  $s \rightarrow +\infty$ ,  $\mathcal{F}_s$  degrades to  $\tilde{\mathcal{F}}$ . In this case,  $\hat{R}(\mathcal{F}_{+\infty}) \leq 2\sqrt{\frac{R}{N}}$ . Note that this bound matches the one that is given in [20]. This is because of the following relation between  $\tilde{\mathcal{F}}$  and the HS of [20],  $\mathcal{F}$ , that is introduced in Section 1: First, let the operator  $A$  in  $\mathcal{F}$  be the identity operator, and then let  $\mathbf{x}$  in  $\mathcal{F}$  be an element of  $\mathcal{H}$ , i.e., let  $\mathbf{x}$  in  $\mathcal{F}$  be  $\phi(\mathbf{x})$  in  $\tilde{\mathcal{F}}$ . Then  $\mathcal{F}$  becomes  $\tilde{\mathcal{F}}$ .

- Obviously, when  $s$  is finite, the bound for  $\mathcal{F}_s$ , which is of order  $O(\frac{1}{T^s} \sqrt{\frac{1}{N}})$ , is more preferred over the aforementioned  $O(\frac{1}{\sqrt{N}})$  bound, as it asymptotically decreases with increasing number of tasks.
- When  $s = \rho^*$ ,  $\hat{R}(\mathcal{F}_{\rho^*}) \leq \frac{2}{T\sqrt{N}} \sqrt{2eR \log T}$ . Here we achieve a bound of order  $O(\frac{\sqrt{\log T}}{T})$ , which decreases faster with increasing  $T$  compared to the bound, when  $s > \rho^*$ .
- When  $s = 1$ ,  $\hat{R}(\mathcal{F}_1) \leq \frac{2}{T\sqrt{N}} \sqrt{2R \log T}$ . While being of order  $O(\frac{\sqrt{\log T}}{T})$ , it features a smaller constant compared to the bound of  $\hat{R}(\mathcal{F}_{\rho^*})$ . In fact, due to the monotonicity of the bound that is given in (11), the tightest bound is obtained when  $s = 1$ .

In the next section, we derive and analyze the generalization bound by letting  $\phi$  to be learned during the training phase.

### 3 Learning the Feature Mapping

In this section, we consider the selection of the feature mapping  $\phi$  during training via an MKL approach. In particular, we will assume that  $\phi = (\sqrt{\theta_1}\phi_1, \dots, \sqrt{\theta_M}\phi_M) \in \mathcal{H}_1 \times \dots \times \mathcal{H}_M$ , where each  $\phi_m : \mathcal{X} \mapsto \mathcal{H}_m$  is selected before training.

#### 3.1 Theoretical Results

Consider the following HS

$$\mathcal{F}_{s,r} \triangleq \{\mathbf{x} \mapsto [\langle \mathbf{w}_1, \phi(\mathbf{x}) \rangle, \dots, \langle \mathbf{w}_T, \phi(\mathbf{x}) \rangle] : \|\mathbf{w}_t\|^2 \leq \lambda_t^2 R, \boldsymbol{\lambda} \in \Omega_s(\boldsymbol{\lambda}), \phi \in \Omega_r(\phi)\} \quad (12)$$

where  $\Omega_r(\phi) = \{\phi : \phi = (\sqrt{\theta_1}\phi_1, \dots, \sqrt{\theta_M}\phi_M), \boldsymbol{\theta} \succeq \mathbf{0}, \|\boldsymbol{\theta}\|_r \leq 1\}$ . By following the same derivation procedure of Lemma 1, we can verify that (7) is also valid for  $\mathcal{F}_{s,r}$ . Therefore, we only need to estimate its ERC. Similar to the previous section, we first give results regarding the monotonicity of  $\hat{R}(\mathcal{F}_{s,r})$ .

**Lemma 3.** Let  $\boldsymbol{\sigma}_t \triangleq [\sigma_t^1, \dots, \sigma_t^N]'$ ,  $\mathbf{u}_t^m \triangleq \boldsymbol{\sigma}_t' \mathbf{K}_t^m \boldsymbol{\sigma}_t$ ,  $\mathbf{u}_t \triangleq [u_t^1, \dots, u_t^M]'$ ,  $v_m \triangleq \sum_{t=1}^T \lambda_t \boldsymbol{\sigma}_t' \mathbf{K}_t^m \boldsymbol{\alpha}_t$ ,  $\mathbf{v} \triangleq [v_1, \dots, v_M]'$ , where  $\mathbf{K}_t^m$  is the kernel matrix that contains elements  $k_m(\mathbf{x}_t^i, \mathbf{x}_t^j)$ . Then  $\forall s \geq 1$  and  $r \geq 1$ ,

$$\hat{R}(\mathcal{F}_{s,r}) = \frac{2}{TN} \sqrt{R} E_{\sigma} \left\{ \sup_{\boldsymbol{\theta} \in \Omega_r(\boldsymbol{\theta})} \sum_{t=1}^T (\boldsymbol{\theta}' \mathbf{u}_t)^{\frac{s}{2}} \right\}^{\frac{1}{s^*}} = \frac{2}{TN} E_{\sigma} \left\{ \sup_{\boldsymbol{\lambda} \in \Omega_s(\boldsymbol{\lambda}), \boldsymbol{\alpha} \in \Omega(\boldsymbol{\alpha})} \|\mathbf{v}\|_{r^*} \right\} \quad (13)$$

where  $\Omega_r(\boldsymbol{\theta}) \triangleq \{\boldsymbol{\theta} : \boldsymbol{\theta} \succeq \mathbf{0}, \|\boldsymbol{\theta}\|_r \leq 1\}$ , and  $\Omega(\boldsymbol{\alpha}) \triangleq \{\boldsymbol{\alpha}_t : \boldsymbol{\sigma}_t' \mathbf{K}_t^m \boldsymbol{\alpha}_t \leq R, \forall t\}$ .

Based on Equation (13), we have the following result:

**Theorem 4.**  $\hat{R}(\mathcal{F}_{s,r})$  is monotonically increasing with respect to  $s$ .

We extend  $\tilde{\mathcal{F}}$  to a MT-MKL setting by letting  $\phi \in \Omega_r(\phi)$ , for  $\phi$  in  $\tilde{\mathcal{F}}$ , which gives  $\tilde{\mathcal{F}}_r \triangleq \{\mathbf{x} \mapsto (\langle \mathbf{w}_1, \phi(\mathbf{x}) \rangle, \dots, \langle \mathbf{w}_T, \phi(\mathbf{x}) \rangle) : \|\mathbf{w}_t\|^2 \leq R, \phi \in \Omega_r(\phi)\}$ . Then, Equation (13) leads to the following result:

**Theorem 5.**  $\hat{R}(\tilde{\mathcal{F}}_r) = \hat{R}(\mathcal{F}_{+\infty,r})$  and, thus,  $\tilde{\mathcal{F}}_r$  is a special case of  $\mathcal{F}_{s,r}$ .

Again, the above results imply that the tightest bound is obtained, when  $s = 1$ . In the following theorem, we provide an upper bound for  $\hat{R}(\mathcal{F}_{s,r})$ .

**Theorem 6.** Let  $\mathcal{F}_{s,r}$  be as defined in Equation (12). Assume that  $\forall \mathbf{x} \in \mathcal{X}$ ,  $m = 1, \dots, M$ ,  $k_m(\mathbf{x}, \mathbf{x}) = \langle \phi_m(\mathbf{x}), \phi_m(\mathbf{x}) \rangle \leq 1$ . The ERC can be bounded as follows:

$$\hat{R}(\mathcal{F}_{s,r}) \leq \frac{2}{T\sqrt{N}} \sqrt{R s^* T^{\frac{2}{s^*}} M^{\max\{\frac{1}{r^*}, \frac{2}{s^*}\}}} \quad (14)$$

The above theorem can be explicitly refined under the following two situations:

**Corollary 1.** *Under the conditions that are given in Theorem 6, we have*

$$\begin{aligned}\hat{R}(\mathcal{F}_{s,r}) &\leq \frac{2}{T\sqrt{N}}\sqrt{\tau RT^{\frac{2}{s^*}} M^{\frac{1}{r^*}}} && \text{if } r^* \leq \log T \\ \hat{R}(\mathcal{F}_{s,r}) &\leq \frac{2}{T\sqrt{N}}\sqrt{\tau RT^{\frac{2}{s^*}} M^{\frac{2}{r^*}}} && \text{if } r^* \geq \log MT\end{aligned}\tag{15}$$

$\forall s \geq 1$ , where  $\tau \triangleq (\max\{s, \rho^*\})^*$ , and

$$\rho \triangleq \begin{cases} 2 \ln T, & r^* \leq \ln T \\ 2 \ln MT, & r^* \geq \ln MT \end{cases}\tag{16}$$

## 3.2 Analysis

Once again, it is worth commenting on the results given in Theorem 6 and Corollary 1:

- Generally,  $\forall s \geq 1$ , (15) gives a bound of order  $O(\frac{1}{T^s})$ . Obviously,  $s \rightarrow +\infty$  is least preferred, since its bound does not decrease with increasing number of tasks. Moreover, based on (14),  $\forall r \geq 1$ ,  $\hat{R}(\mathcal{F}_{1,r})$ 's bound is of order  $O(\sqrt{M^{\frac{1}{r^*}}})$ . Compared to the  $O(\sqrt{M^{\frac{1}{r^*}} \min(\lceil \log M \rceil, \lceil r^* \rceil)})$  bound of single-task MKL scenario, which is examined in [15], our bound for MT-MKL is tighter, for almost all  $M$ , when  $r$  is small, which is usually a preferred setting.
- When  $r^* \geq \log MT$ , the bound given in (15) is monotonically increasing with respect to  $s$ . When  $s = \rho^*$ , we have  $\hat{R}(\mathcal{F}_{\rho^*,r}) \leq \frac{2}{T\sqrt{N}}\sqrt{2eR \log MT}$ . This gives a  $O(\frac{\sqrt{\log MT}}{T})$  bound. Note that it is proved that the best bound that can be obtained in single-task multiple kernel classification is of order  $O(\sqrt{\log M})$  [6]. Obviously, this logarithmic bound is preserved in the MT-MKL context. When  $s$  further decreases to 1, we have  $\hat{R}(\mathcal{F}_{1,r}) \leq \frac{2}{T\sqrt{N}}\sqrt{2RM^{\frac{1}{\log MT}} \log MT}$ . Since  $M^{\frac{1}{\log MT}}$  can never be larger than  $e$ , this bound is even tighter than the one obtained, when  $s = \rho^*$ .
- When  $r^* \leq \log T$ , the bound that is given in (15) is monotonically increasing with respect to  $s$ . When  $s = \rho^*$ , we have  $\hat{R}(\mathcal{F}_{\rho^*,r}) \leq \frac{2}{T\sqrt{N}}\sqrt{2eRM^{\frac{1}{r^*}} \log T}$ . This gives a  $O(\frac{\sqrt{M^{\frac{1}{r^*}} \log T}}{T})$  bound. When  $s$  further decreases to 1, we have  $\hat{R}(\mathcal{F}_{1,r}) \leq \frac{2}{T\sqrt{N}}\sqrt{2RM^{\frac{1}{r^*}} \log T}$ . As we can see, it further decreases the bound by a constant factor  $e$ .
- Compared to the optimum bounds that are given in the previous two situations, *i.e.*,  $r^* \geq \log MT$  and  $r^* \leq \log T$ , we can see that, when  $r^* \geq \log MT$ , we achieve a better bound with respect to  $M$ , *i.e.*,  $O(\sqrt{\log M})$  versus  $O(\sqrt{M^{\frac{1}{r^*}}})$ . On the other hand, with regards to  $T$ , even though we get a  $O(\frac{\sqrt{\log T}}{T})$  bound in both cases, the case of  $r^* \leq \log T$  features a lower constant factor.

To summarize, MT-MKL not only preserves the optimal  $O(\sqrt{\log M})$  bound encountered in single-task MKL, but also preserves the optimal  $O(\frac{\sqrt{\log T}}{T})$  bound encountered in the single-kernel MTL case, which was given in the previous section.

## 4 Discussion

### 4.1 Relation to Group-Lasso type regularizer

In the next theorem, we show the relation between our HS and the one that is based on Group-Lasso type regularizer.

**Theorem 7.** *The HS  $\mathcal{F}_s$  is equivalent to*

$$\mathcal{F}_s^{GL} \triangleq \{\mathbf{x} \mapsto [\langle \mathbf{w}_1, \phi(\mathbf{x}) \rangle, \dots, \langle \mathbf{w}_T, \phi(\mathbf{x}) \rangle]': (\sum_{t=1}^T \|\mathbf{w}_t\|^s)^{\frac{2}{s}} \leq R\} \quad (17)$$

*Similarly,  $\mathcal{F}_{s,r}$  is equivalent to*

$$\mathcal{F}_{s,r}^{GL} \triangleq \{\mathbf{x} \mapsto [\langle \mathbf{w}_1, \tilde{\phi}(\mathbf{x}) \rangle, \dots, \langle \mathbf{w}_T, \tilde{\phi}(\mathbf{x}) \rangle]': (\sum_{t=1}^T \|\mathbf{w}_t\|^s)^{\frac{2}{s}} \leq R, \boldsymbol{\theta} \in \Omega_r(\boldsymbol{\theta})\} \quad (18)$$

where  $\|\mathbf{w}_t\|^2 = \sum_{m=1}^M \frac{\|\mathbf{w}_t^m\|^2}{\theta_m}$ ,  $\tilde{\phi} = (\phi_1, \dots, \phi_M)$ ,  $\Omega_r(\boldsymbol{\theta}) = \{\boldsymbol{\theta} : \boldsymbol{\theta} \succeq \mathbf{0}, \|\boldsymbol{\theta}\|_r \leq 1\}$ .

Obviously, by employing the Group-Lasso type regularizer, one can obtain the HSs that are proposed in previous sections. Below is a Regularization-Loss framework based on this regularizer with pre-selected kernel:

$$\min_{\mathbf{w}_1, \dots, \mathbf{w}_T} (\sum_{t=1}^T \|\mathbf{w}_t\|^s)^{\frac{2}{s}} + C \sum_{i,t} L(\langle \mathbf{w}_t, \phi(\mathbf{x}_t^i) \rangle, y_t^i) \quad (19)$$

The MKL-based model can be similarly defined.

## 4.2 Other related works

There has been substantial efforts put on the research of kernel-based MTL and also MT-MKL. We in this subsection discuss four closely related papers, and emphasize the difference between this paper and these works.

First, we consider [1] and [24]. Both of these two papers consider Group-Lasso type regularizer to achieve different level of sparsity. Specifically, [1] utilized the regularizer

$$(\sum_{j=1}^n (\sum_{k=1}^{n_j} \|\mathbf{w}_{jk}\|)^s)^{\frac{2}{s}}, s \geq 2 \quad (20)$$

where  $l_1$  norm regularization is applied to the weights of each of the  $n$  groups (*i.e.* the inner summation), and the group-wise regularization is achieved via  $l_s$  norm regularizer. It is hoped that by utilizing this regularizer, one can achieve inner-group sparsity and group-wise non-sparsity. This regularizer can be applied to MT-MKL, by letting  $\mathbf{w}_{jk}$  to be  $\mathbf{w}_t^m$ , which yields the regularizer

$$(\sum_{t=1}^T (\sum_{m=1}^M \|\mathbf{w}_t^m\|)^s)^{\frac{2}{s}}, s \geq 2 \quad (21)$$

This is similar to the one that appeared in  $\mathcal{F}_{s,r}^{GL}$ . However, the major difference between our regularizer and (21) is that, in  $\mathcal{F}_{s,r}^{GL}$ , instead of applying an  $l_1$  norm to the inner summation, we used  $\sum_{m=1}^M \frac{\|\mathbf{w}_t^m\|^2}{\theta_m}$ , where  $\theta_m$  has a feasible region that is parametrized by  $r$ . Therefore, our regularizer encompasses MT-MKL with common kernel function, which is learned during training, while (21) does not.

In [24], the authors considered

$$\sum_{m=1}^M (\sum_{t=1}^T \|\mathbf{w}_t^m\|^q)^{\frac{2}{q}}, 0 \leq p \leq 1, q \geq 1 \quad (22)$$

By applying the  $l_p$  (pseudo-)norm, the authors intended to achieve sparsity over the outer summation, while variable sparsity is obtained for the inner summation, due to the  $l_q$  norm. The major difference between (22) and  $\mathcal{F}_{s,r}^{GL}$  are twofold. First, the order of the double summation is different, *i.e.*, in (22), the  $\mathbf{w}_t^m$ 's that belong to the same RKHS is considered as a group, while  $\mathcal{F}_{s,r}^{GL}$  treats each task as a group. Second, similar to the reason that is discussed above, (22) does not encompass the MT-MKL with common kernel function, which is learned during the training phase.

In the following, we discuss the difference between our work and the two theoretical works, [22] and [13], which derived generalization bound of the HSs that are similar to ours. In [22], the authors consider the regularizer

$$\|\mathbf{w}\|_{\mathcal{M}} \triangleq \inf\left\{ \sum_{M \in \mathcal{M}} \|\mathbf{v}_M\| : \mathbf{v}_M \in \mathcal{H}, \sum_{M \in \mathcal{M}} M\mathbf{v}_M = \mathbf{w} \right\} \quad (23)$$

where  $\mathcal{M}$  is an almost countable set of symmetric bounded linear operators on  $\mathcal{H}$ . This general form covers several regularizers, such as Lasso, Group-Lasso, weighted Group-Lasso, etc. A key observation is that, in order for a specific regularizer to be covered by this general expression, the regularizer needs to be either summation of several norms, or the infimum of such a summation over a feasible region. For our regularizer  $(\sum_{t=1}^T \|\mathbf{w}_t\|^s)^{\frac{2}{s}}$ , obviously, it is not summation of norms (note the power outside the summation). Also, it is not immediately clear, if it can be represented by an infimum, which we just mentioned. Therefore, it appears that there is no succinct way to represent our regularizer as a special case of (23) and the same seems to be the case for our MT-MKL regularizer.

Also, for our HSs, it is clear how the generalization bounds relate to the number of tasks  $T$  and number of kernels  $M$ , in  $\mathcal{F}_s$  and  $\mathcal{F}_{s,r}$ , and under which circumstances the logarithmic bound can be achieved. This observation may be hard to obtain from the bound that is derived in (23), even though one may view our regularizers as special cases of (23).

In [13], the authors derived generalization bound for regularization-based MTL models, with regularizer  $\|\mathbf{W}\|_{r,p} \triangleq \|(\|\mathbf{w}^1\|_r, \dots, \|\mathbf{w}^n\|_r)\|_p$ . However, their work assumes  $\mathbf{W} \in \mathbb{R}^{m \times n}$ , while we assume our  $\mathbf{w}_t$ 's be vectors of a potentially infinite-dimensional Hilbert space. Also, such group norm does not generalize our MT-MKL regularizer, therefore their bound cannot be applied to our HS, even if their results were to be extended to infinite-dimensional vector spaces.

## 5 Experiments

In this section, we investigate via experimentation the generalization bounds of our HSs. We first evaluate the discrepancy between the ERC of  $\mathcal{F}_s$ ,  $\mathcal{F}_{s,r}$  and their bounds. We show experimentally that the bound gives a good estimate of the relevant ERC. Then, we consider a new SVM-based MTL model that uses  $\mathcal{F}_s$  as its HS. The model is subsequently extended to allow for MT-MKL by using  $\mathcal{F}_{s,r}$  as its HS.

### 5.1 ERC Bound Evaluation

For  $\mathcal{F}_s$ , given a data set and a pre-selected kernel function, we can calculate its kernel matrices  $\mathbf{K}_t, t = 1, \dots, T$ . Then, the ERC is given by Equation (10). In order to approximate the expectation  $E_{\sigma}\{\|\mathbf{u}\|_{s^*}\}$ , we resort to Monte Carlo simulation by drawing a large number,  $D$ , of i.i.d samples for the  $\sigma_t$ 's from a uniform distribution on the hyper-cube  $\{-1, 1\}^N$ . Subsequently, for each sample we evaluate the argument of the expectation and average the results. For  $\mathcal{F}_{s,r}$ , the ERC is calculated as in the first equation of (13). For each of the  $D$  samples of  $\sigma_t$ , we can calculate the corresponding  $\mathbf{u}_t$ . Then, we solve the maximization problem by using CVX [11, 12]. Finally, we calculate the average of the  $D$  values to approximate the ERC. For the experiment related to  $\mathcal{F}_{s,r}$ , we only considered the case, when  $s \geq 2$ . Under these circumstances, the maximization problem in (13) is concave and can be easily solved, unlike the case, when  $s \in [1, 2)$ .

We used the Letter data set <sup>1</sup> for this set of experiments. It is a collection of handwritten words compiled by Rob Kassel of the MIT Spoken Language Systems Group. The associated MTL problem involves 8 tasks, each of which is a binary classification problem for handwritten letters. The 8 tasks are: 'C' vs. 'E', 'G' vs. 'Y', 'M' vs. 'N', 'A' vs. 'G', 'I' vs. 'J', 'A' vs. 'O', 'F' vs. 'T' and 'H' vs. 'N'. Each letter is represented by a  $8 \times 16$  pixel image, which forms a 128-dimensional feature vector. We chose 100 samples for each letter, and set  $D = 10^4$ . To calculate the kernel matrix, we used a Gaussian kernel with spread parameter  $2^7$  for  $\mathcal{F}_s$ , and 9 different Gaussian kernels with spreads  $\{2^{-7}, 2^{-5}, 2^{-3}, 2^{-1}, 2^0, 2^1, 2^3, 2^5, 2^7\}$  for  $\mathcal{F}_{s,r}$ . Finally,  $R$  was set to 1.

The experimental results are shown in Figure 1. In both sub-figures, it is obvious that both our bound and the real ERC are monotonically increasing. For  $\mathcal{F}_s$ , it can be seen that the bound is tight everywhere.

<sup>1</sup>Available at: <http://www.cis.upenn.edu/~taskar/ocr/>



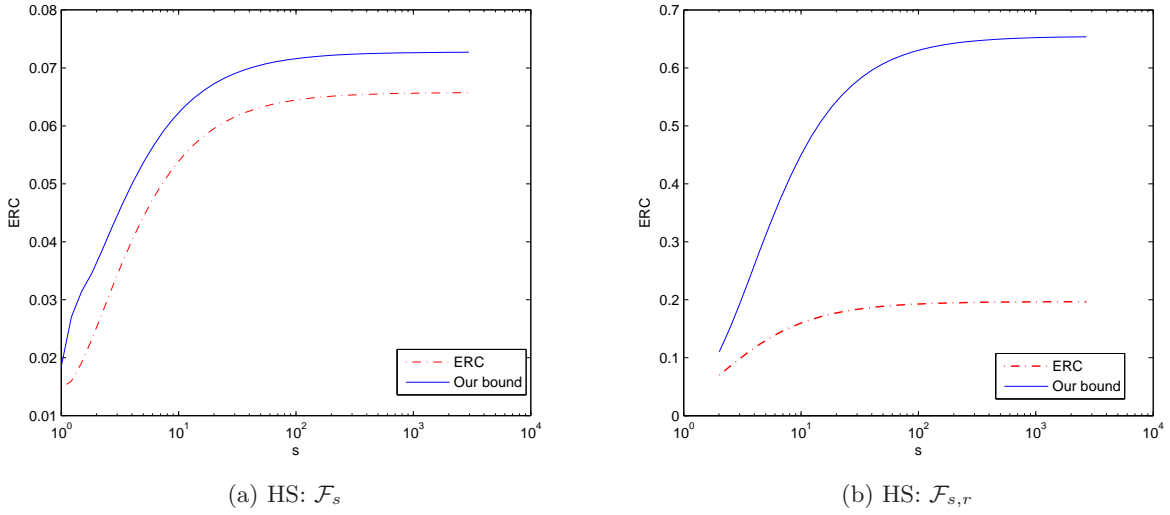


Figure 1: Comparison between Monte Carlo-estimated ERCs and our derived bounds using the Letter data set.  $10^4$   $\sigma_t$  samples were used for Monte Carlo estimation. We sampled 100 data for each letter and used 9 kernel functions in multiple kernel scenario.

For  $\mathcal{F}_{s,r}$ , even though the difference between our bound and the Monte Carlo estimated ERC becomes larger when  $s$  grows, the bound is still tight for small  $s$ . This experiment shows a good match between the real ERC and our bound, which verifies our theoretical analysis in Section 2 and Section 3.

## 5.2 SVM-based Model

In this subsection we present a new SVM-based model which reflects our proposed HS. For training data  $\{\mathbf{x}_t^i, y_t^i\} \in \mathcal{X} \times \{-1, 1\}, i = 1, \dots, N_t, t = 1, \dots, T$  and fixed feature mapping  $\phi: \mathcal{X} \mapsto \mathcal{H}$ , our model is given as follows:

$$\begin{aligned} \min_{\mathbf{w}, \boldsymbol{\xi}, b} & \left( \sum_{t=1}^T \left( \frac{\|\mathbf{w}_t\|^2}{2} \right)^{\frac{s}{2}} \right)^{\frac{2}{s}} + C \sum_{t,i=1}^{T, N_t} \xi_t^i \\ \text{s.t.} & y_t^i (\langle \mathbf{w}_t, \phi(\mathbf{x}_t^i) \rangle + b_t) \geq 1 - \xi_t^i, \quad \xi_t^i \geq 0, \forall i, t \end{aligned} \quad (24)$$

Obviously,  $\mathcal{F}_s$  is the HS of (24). Such minimization problem can be solved as follows. First, note that when  $1 \leq s \leq 2$ , the problem is equivalent to

$$\begin{aligned} \min_{\mathbf{w}, \boldsymbol{\xi}, b, \boldsymbol{\lambda}} & \sum_{t=1}^T \frac{\|\mathbf{w}_t\|^2}{2\lambda_t} + C \sum_{t,i=1}^{T, N_t} \xi_t^i \\ \text{s.t.} & y_t^i (\langle \mathbf{w}_t, \phi(\mathbf{x}_t^i) \rangle + b_t) \geq 1 - \xi_t^i, \quad \xi_t^i \geq 0, \forall i, t \\ & \boldsymbol{\lambda} \succeq \mathbf{0}, \|\boldsymbol{\lambda}\|_{\frac{s}{2-s}} \leq 1 \end{aligned} \quad (25)$$

which can be easily solved via block coordinate descent method, with  $\{\mathbf{w}, \boldsymbol{\xi}, b\}$  as a group and  $\boldsymbol{\lambda}$  as another. When  $s > 2$ , (24) is equivalent to

$$\begin{aligned} \min_{\mathbf{w}, \boldsymbol{\xi}, b} \max_{\boldsymbol{\lambda}} & \sum_{t=1}^T \frac{\lambda_t \|\mathbf{w}_t\|^2}{2} + C \sum_{t,i=1}^{T, N_t} \xi_t^i \\ \text{s.t.} & y_t^i (\langle \mathbf{w}_t, \phi(\mathbf{x}_t^i) \rangle + b_t) \geq 1 - \xi_t^i, \quad \xi_t^i \geq 0, \forall i, t \\ & \boldsymbol{\lambda} \succeq \mathbf{0}, \|\boldsymbol{\lambda}\|_{\frac{s}{s-2}} \leq 1 \end{aligned} \quad (26)$$

Since it is a convex-concave min-max problem with compact feasible region, the order of min and max can be interchanged [25], which gives the objective function

$$\max_{\lambda} \min_{\mathbf{w}, \xi, b} \sum_{t=1}^T \lambda_t \left( \frac{\|\mathbf{w}_t\|^2}{2} + \frac{C}{\lambda_t} \sum_{i=1}^{N_t} \xi_t^i \right) \quad (27)$$

Calculating the dual form of the inner SVM problem gives the following maximization problem:

$$\begin{aligned} \max_{\alpha, \lambda} \quad & \sum_{t=1}^T \lambda_t \left( \alpha_t' \mathbf{1} - \frac{1}{2} \alpha_t' \mathbf{Y}_t \mathbf{K}_t \mathbf{Y}_t \alpha_t \right) \\ \text{s.t.} \quad & \mathbf{0} \preceq \alpha_t \preceq \frac{C}{\lambda_t} \mathbf{1}, \quad \alpha_t' \mathbf{y}_t = 0, \quad \forall t \\ & \lambda \succeq \mathbf{0}, \quad \|\lambda\|_{\frac{s}{s-2}} \leq 1 \end{aligned} \quad (28)$$

where  $\mathbf{Y}_t \triangleq \text{diag}([y_t^1, \dots, y_t^{N_t}]')$  and  $\mathbf{K}_t$  is the kernel matrix that is calculated based on the training data from the  $t$ -th task. Group coordinate descent can be utilized to solve (28), with  $\lambda$  as a group and  $\alpha$  as another group.

The model can be extended so that it can accommodate MKL as follows:

$$\begin{aligned} \min_{\mathbf{w}_t, \xi_t, b_t, \theta} \quad & \left( \sum_{t=1}^T \left( \sum_{m=1}^M \frac{\|\mathbf{w}_t^m\|^2}{2\theta_m} \right)^{\frac{s}{2}} \right)^{\frac{2}{s}} + C \sum_{t=1}^{T, N_t} \xi_t^i \\ \text{s.t.} \quad & y_t^i (\langle \mathbf{w}_t, \phi(\mathbf{x}_t^i) \rangle + b_t) \geq 1 - \xi_t^i, \quad \xi_t^i \geq 0, \quad \forall i, t \\ & \theta \succeq \mathbf{0}, \quad \|\theta\|_r \leq 1 \end{aligned} \quad (29)$$

where  $\phi = (\phi_1, \dots, \phi_M)$ . Obviously, its HS is  $\mathcal{F}_{s,r}$ . This model can be solved via the similar strategy of solving (24). The only situation that needs a different algorithm is the case when  $s > 2$ , where (29) will be transformed to

$$\begin{aligned} \min_{\theta} \max_{\alpha, \lambda} \quad & \sum_{t=1}^T \lambda_t \left( \alpha_t' \mathbf{1} - \frac{1}{2} \alpha_t' \mathbf{Y}_t \left( \sum_{m=1}^M \theta_m \mathbf{K}_t^m \right) \mathbf{Y}_t \alpha_t \right) \\ \text{s.t.} \quad & \mathbf{0} \preceq \alpha_t \preceq \frac{C}{\lambda_t} \mathbf{1}, \quad \alpha_t' \mathbf{y}_t = 0, \quad \forall t \\ & \lambda \succeq \mathbf{0}, \quad \|\lambda\|_{\frac{s}{s-2}} \leq 1 \\ & \theta \succeq \mathbf{0}, \quad \|\theta\|_r \leq 1 \end{aligned} \quad (30)$$

This min-max problem cannot be solved via group coordinate descent. Instead, we use the Exact Penalty Function method to solve it. We omit the details of this method and refer the readers to [27], since it is not the focus of this paper.

### 5.3 Experimental Results on the SVM-based model

We performed our experiments on two well-known and frequently-used multi-task data sets, namely Letter and Landmine, and two handwritten digit data sets, namely MNIST and USPS. The Letter data set was described in the previous sub-section. Due to the large size of the original Letter data set, we randomly sampled 200 points for each letter to construct a training set. One exception is the letter  $j$ , as it contains only 189 samples in total. The Landmine data set<sup>2</sup> consists of 29 binary classification tasks. Each datum is a 9-dimensional feature vector extracted from radar images that capture a single region of landmine fields. Tasks 1 – 15 correspond to regions that are relatively highly foliated, while the other 14 tasks correspond to regions that are bare earth or desert. The tasks entail different amounts of data, varying from 30 to 96 samples. The goal is to detect landmines in specific regions.

<sup>2</sup>Available at: <http://people.ee.duke.edu/~lcarin/LandmineData.zip>

Regarding the MNIST<sup>3</sup> and USPS<sup>4</sup> data sets, each of the two are grayscale images containing hand-written digits from 0 to 9 with 784 and 256 features respectively. As was the case with the Letter data set, due to the large size of the original data set, we randomly sampled 100 data from each digit population to form a training set consisting of 1000 samples in total. To simulate the MTL scenario, we split the data into 45 binary classification tasks by applying a one-versus-one strategy. The classification accuracy was then calculated as the average of classification accuracies over all tasks.

For all our experiments, the training set size was set to 10% of the available data. We did not choose large training sets, since, as we can see from the generalization bound in (11), (14) and (15), when  $N$  is large, the effect of  $s$  becomes minor. For MT-MKL, we chose the 9 Gaussian kernels that were introduced in Section 5.1, as well as a linear and a  $2^{nd}$ -order polynomial kernel. For the single kernel case, we selected the optimal kernel from these 11 kernel function candidates via cross-validation. SVM’s regularization parameter  $C$  was selected from the set  $\{1/81, 1/27, 1/9, 1/3, 1, 3, 9, 27, 81\}$ . In the MT-MKL case, the norm parameter  $r$  for  $\theta$  was set to 1 to induce sparsity on  $\theta$ . We varied  $s$  from 1 to 100, and reported the best average classification accuracy over 20 runs. For  $s > 100$ , the results are almost always the same as that when  $s = 100$ , therefore we did not report these results. In fact, as show below, the model performance deteriorates quickly when  $s > 2$ , and changes very few when  $s > 10$ . The experimental results are given in Figure 2.

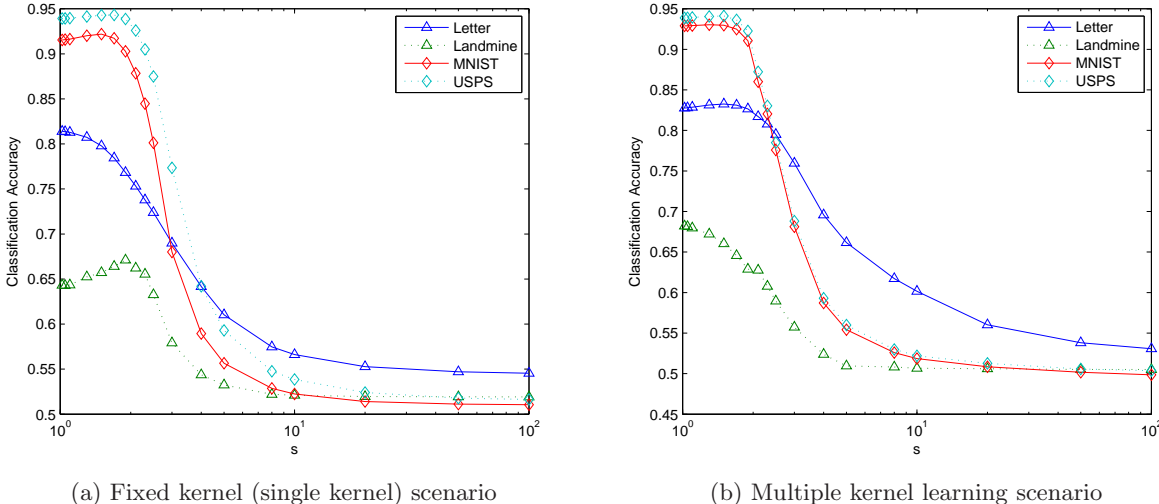


Figure 2: Average classification accuracy on 20 runs for different  $s$  values

It can be seen that, the classification accuracy is roughly monotonically decreasing with respect to  $s$ , and the performance deteriorates significantly when  $s > 2$ . In many situations, the best performance is achieved, when  $s = 1$ . This result supports our theoretical analysis that the lowest generalization bound is obtained when  $s = 1$ . On the other hand, in some situations, such as the cases which consider the USPS data set in a single kernel setting, and the Letter data set in multiple kernel setting, the optimum model is not obtained when  $s = 1$ . This seems contradictory to our previously stated claims. However, this phenomenon can be explained similarly to the discussion in Section 5.1 of [15], which we summarize here: Obviously, for different  $s$ , the optimal solution ( $f_t$ 's) may be different. To get the optimal solution, we need to tune the “size” of the HS, such that the optimum  $f_t$ 's are contained in the HS. This implies that the size of the HS, which is parametrized by  $R$ , could be different for different  $s$ , instead of being fixed as discussed in previous sections. It is possible that the HS size (thus  $R$ ) is very small, when  $s \neq 1$ . In this scenario, the lowest bound could be obtained when  $s \neq 1$ . For a more detailed discussion, we refer the reader to Section 5.1 in [15]. Finally, it is interesting to see how the performance deteriorates when  $s$  becomes large. The reason for the bad performance is as follows. Observe that the regularizer is the  $l_{\frac{s}{2}}$  norm of the  $T$  SVM regularizers. Consider

<sup>3</sup>Available at: <http://yann.lecun.com/exdb/mnist/>

<sup>4</sup>Available at: <http://www.cs.nyu.edu/~roweis/data.html>

the extreme case, when  $s \rightarrow \infty$ , the  $l_{\frac{s}{2}}$  norm becomes the  $l_{\infty}$  norm, which is  $\max_t \{\frac{\|\mathbf{w}_t\|^2}{2}\}$ . In this scenario, the regularizer of the model is only the one which has the smallest margin, while the regularizers of other tasks are ignored. Therefore, it is not a surprise that the performance of the other tasks is bad, which leads to low average classification accuracy. For large  $s$  value, even though it is not infinity, the bad result can be similarly analyzed.

## 6 Conclusions

In this paper, we proposed a Multi-Task Learning (MTL) Hypothesis Space (HS)  $\mathcal{F}_s$  involving  $T$  discriminative functions parametrized by weights  $\mathbf{w}_t$ . The weights are controlled by norm-ball constraints, whose radii are variable and estimated during the training phase. It extends an HS  $\tilde{\mathcal{F}}$  that has been previously investigated in the literature, where the radii are pre-determined. It is shown that the latter space is a special case of  $\mathcal{F}_s$ , when  $s \rightarrow +\infty$ . We derived and analyzed the generalization bound of  $\mathcal{F}_s$  and have shown that the bound is monotonically increasing with respect to  $s$ . Also, in the optimal case ( $s = 1$ ), a bound of order  $O(\frac{\sqrt{\log T}}{T})$  is achieved. We further extended the HS to  $\mathcal{F}_{s,r}$ , which is suitable for Multi-Task Multiple Kernel Learning (MT-MKL). Similar results were obtained, including a bound that is monotonically increasing with  $s$  and an optimal bound of order  $O(\frac{\sqrt{\log MT}}{T})$ , when  $s = 1$ . The experimental results shown that our Empirical Rademacher Complexity (ERC) bound is tight and matches the real ERC very well. We then demonstrated the relation between our HS and the Group-Lasso type regularizer, and a Support Vector Machine (SVM)-based model was proposed with HS  $\mathcal{F}_s$ , that was further extended to handle MT-MKL by using the HS  $\mathcal{F}_{s,r}$ . The experimental results on multi-task classification data sets showed that the classification accuracy is monotonically decreasing with respect to  $s$ , and the optimal results for most experiments are indeed achieved, when  $s = 1$ , as indicated by our analysis. The presence of results that, contrary to our analysis, are optimal, when  $s \neq 1$ , can be justified similarly to Section 5.1 in [15].

## Acknowledgments

C. Li acknowledges partial support from National Science Foundation (NSF) grant No. 0806931. Moreover, M. Georgiopoulos acknowledges partial support from NSF grants No. 0525429, No. 0963146, No. 1200566 and No. 1161228. Finally, G. C. Anagnostopoulos acknowledges partial support from NSF grants No. 0717674 and No. 0647018. Any opinions, findings, and conclusions or recommendations expressed in this material are those of the authors and do not necessarily reflect the views of the NSF.

## References

- [1] Jonathan Aflalo, Aharon Ben-Tal, Chiranjib Bhattacharyya, Jagarlapudi Saketha Nath, and Sankaran Raman. Variable sparsity kernel learning. *Journal of Machine Learning Research*, 12:565–592, 2011.
- [2] Andreas Argyriou, Theodoros Evgeniou, and Massimiliano Pontil. Convex multi-task feature learning. *Machine Learning*, 73:243–272, 2008.
- [3] Andrea Caponnetto, Charles A. Micchelli, Massimiliano Pontil, and Yiming Ying. Universal multi-task kernels. *Journal of Machine Learning Research*, 9:1615–1646, 2008.
- [4] Rich Caruana. Multitask learning. *Machine Learning*, 28:41–75, 1997.
- [5] Jianhui Chen, Jiayu Zhou, and Jieping Ye. Integrating low-rank and group-sparse structures for robust multi-task learning. In *KDD*, 2011.
- [6] Corinna Cortes, Mehryar Mohri, and Afshin Rostamizadeh. Generalization bounds for learning kernels. In *ICML*, 2010.
- [7] Theodoros Evgeniou, Charles A. Micchelli, and Massimiliano Pontil. Learning multiple tasks with kernel methods. *Journal of Machine Learning Research*, 6:615–637, 2005.

- [8] Hongliang Fei and Jun Huan. Structured feature selection and task relationship inference for multi-task learning. In *ICDM*, 2011.
- [9] Mehmet Gonen and Ethem Alpaydin. Multiple kernel learning algorithms. *Journal of Machine Learning Research*, 12:2211–2268, 2011.
- [10] Pinghua Gong, Jieping Ye, and Changshui Zhang. Multi-stage multi-task feature learning. In *NIPS*, 2012.
- [11] M. Grant and S. Boyd. Graph implementations for nonsmooth convex programs. In V. Blondel, S. Boyd, and H. Kimura, editors, *Recent Advances in Learning and Control*, Lecture Notes in Control and Information Sciences, pages 95–110. Springer-Verlag Limited, 2008.
- [12] M. Grant and S. Boyd. CVX: Matlab software for disciplined convex programming, version 1.21, April 2011.
- [13] Sham M. Kakade, Shai Shalev-Shwartz, and Ambuj Tewari. Regularization techniques for learning with matrices. *Journal of Machine Learning Research*, 13:1865–1890, 2012.
- [14] Zhuoliang Kang, Kristen Grauman, and Fei Sha. Learning with whom to share in multi-task feature learning. In *ICML*, 2011.
- [15] Marius Kloft, Ulf Brefeld, Soren Sonnenburg, and Alexander Zien.  $l_p$ -norm multiple kernel learning. *Journal of Machine Learning Research*, 12:953–997, 2011.
- [16] Mladen Kolar and Han Liu. Marginal regression for multitask learning. In *NIPS*, 2012.
- [17] Stanislaw Kwapien and Wojbor A. Woyczynski. *Random Series and Stochastic Integrals: Single and Multiple*. Birkhauser, 1992.
- [18] Gert R. G. Lanckriet, Nello Cristianini, Peter Bartlett, Laurent El Ghaoui, and Michael I. Jordan. Learning the kernel matrix with semidefinite programming. *J. Mach. Learn. Res.*, 5:27–72, December 2004.
- [19] Aurelie C. Lozano and Grzegorz Swirszcz. Multi-level lasso for sparse multi-task regression. In *NIPS*, 2012.
- [20] Andreas Maurer. Bounds for linear multi-task learning. *Journal of Machine Learning Research*, 7:117–139, 2006.
- [21] Andreas Maurer. The rademacher complexity of linear transformation classes. In Gbor Lugosi and HansUlrich Simon, editors, *Learning Theory*, volume 4005 of *Lecture Notes in Computer Science*, pages 65–78. Springer Berlin Heidelberg, 2006. doi:10.1007/11776420\_8.
- [22] Andreas Maurer and Massimiliano Pontil. Structured sparsity and generalization. *Journal of Machine Learning Research*, 13:671–690, 2012.
- [23] Shibir Parameswaran and Kilian Q. Weinberger. Large margin multi-task metric learning. In *NIPS*, 2012.
- [24] Alain Rakotomamonjy, Remi Flamary, Gilles Gasso, and Stephane Canu.  $l_p - l_q$  penalty for sparse linear and sparse multiple kernel multitask learning. *IEEE Transactions on Neural Networks*, 22:1307–1320, 2011.
- [25] M. Sion. On general minimax theorems. *Pacific Journal of Mathematics*, 8:171–176, 1958.
- [26] Lei Tang, Jianhui Chen, and Jieping Ye. On multiple kernel learning with multiple labels. In *IJCAI*, 2009.
- [27] G.A. Watson. Globally convergent methods for semi-infinite programming. *BIT Numerical Mathematics*, 21:392–373, 1981.

- [28] Yu Zhang and Dit-Yan Yeung. Transfer metric learning by learning task relationships. In *KDD*, 2010.
- [29] Leon wenliang Zhong and James T. Kwok. Convex multitask learning with flexible task clusters. In *ICML*, 2012.

## 7 Appendix

### 7.1 Preliminaries

In this subsection, we provide two results that will be used in the following subsections.

**Lemma 4.** *Let  $p \geq 1$ ,  $\mathbf{x}, \mathbf{a} \in \mathbb{R}^n$  such that  $\mathbf{a} \succeq \mathbf{0}$  and  $\mathbf{a} \neq \mathbf{0}$ . Then,*

$$\max_{\mathbf{x} \in \Omega(\mathbf{x})} \mathbf{a}'\mathbf{x} = \|\mathbf{a}\|_p \quad (31)$$

where  $\Omega(\mathbf{x}) \triangleq \{\mathbf{x} : \|\mathbf{x}\|_{p^*} \leq 1\}$ .

This lemma can be simply proved by utilizing Lagrangian multiplier method with respect to the maximization problem.

**Lemma 5.** *Let  $\mathbf{x}_1, \dots, \mathbf{x}_n \in \mathcal{H}$ , then we have that*

$$E_\sigma \left\| \sum_{i=1}^n \sigma_i \mathbf{x}_i \right\|^p \leq \left( p \sum_{i=1}^n \|\mathbf{x}_i\|^2 \right)^{\frac{p}{2}} \quad (32)$$

for any  $p \geq 1$ , where  $\sigma_i$ 's are the Rademacher-distributed random variables.

For  $1 \leq p < 2$ , the above result can be simply proved using Lyapunov's inequality. When  $p \geq 2$ , the lemma can be proved by using Proposition 3.3.1 and 3.4.1 in [17].

### 7.2 Proof to Lemma 2

*Proof.* First notice that  $\mathcal{F}_s$  is equivalent to the following HS:

$$\mathcal{F}_s \triangleq \{\mathbf{x} \mapsto (\lambda_1 \langle \mathbf{w}_1, \phi(\mathbf{x}) \rangle, \dots, \lambda_T \langle \mathbf{w}_T, \phi(\mathbf{x}) \rangle)' : \|\mathbf{w}_t\|^2 \leq R, \boldsymbol{\lambda} \in \Omega_s(\boldsymbol{\lambda})\} \quad (33)$$

According to the same reasoning of Equations (1) and (2) in [6], we know that  $\mathbf{w}_t = \sum_{i=1}^N \alpha_t^i \phi(\mathbf{x}_t^i)$ , and the constraint  $\|\mathbf{w}_t\|^2 \leq R$  is equivalent to  $\boldsymbol{\alpha}_t' \mathbf{K}_t \boldsymbol{\alpha}_t \leq R$ . Therefore, based on the definition of ERC that is given in Equation (8), we have that

$$\hat{R}(\mathcal{F}_s) = \frac{2}{TN} E_\sigma \left\{ \sup_{\boldsymbol{\alpha}_t \in \mathcal{F}_s} \sum_{t=1}^T \lambda_t \boldsymbol{\sigma}_t' \mathbf{K}_t \boldsymbol{\alpha}_t \right\} \quad (34)$$

where  $\mathcal{F}_s = \{\boldsymbol{\alpha}_t \mid \boldsymbol{\alpha}_t' \mathbf{K}_t \boldsymbol{\alpha}_t \leq \lambda_t^2 R, \forall t; \boldsymbol{\lambda} \in \Omega_s(\boldsymbol{\lambda})\}$ . To solve the maximization problem with respect to  $\boldsymbol{\alpha}_t$ , we observe that the  $T$  problems are independent and thus can be solved individually. Based on Cauchy-Schwartz inequality, the optimal  $\boldsymbol{\alpha}_t$  is achieved when  $\mathbf{K}_t^{\frac{1}{2}} \boldsymbol{\alpha}_t = c_t \mathbf{K}_t^{\frac{1}{2}} \boldsymbol{\sigma}_t$  where  $c_t$  is a constant.

Substituting this result into each of the  $T$  maximization problems, we have the following:

$$\begin{aligned} \max_{c_t} \quad & c_t \boldsymbol{\sigma}_t' \mathbf{K}_t \boldsymbol{\sigma}_t \\ \text{s.t.} \quad & c_t^2 \boldsymbol{\sigma}_t' \mathbf{K}_t \boldsymbol{\sigma}_t \leq R \end{aligned} \quad (35)$$

Obviously, the optimal  $c_t$  is obtained when  $c_t = \sqrt{\frac{R}{\boldsymbol{\sigma}_t' \mathbf{K}_t \boldsymbol{\sigma}_t}}$ . Therefore the ERC becomes now

$$\hat{R}(\mathcal{F}_s) = \frac{2}{TN} E_\sigma \left\{ \sup_{\boldsymbol{\lambda} \in \Omega_s(\boldsymbol{\lambda})} \sum_{t=1}^T \lambda_t \sqrt{\boldsymbol{\sigma}_t' \mathbf{K}_t \boldsymbol{\sigma}_t R} \right\} \quad (36)$$

Since  $s \geq 1$ , based on Lemma 4, it is not difficult to get the solution of the maximization problem with respect to  $\lambda$ , which gives

$$\begin{aligned}\hat{R}(\mathcal{F}_s) &= \frac{2\sqrt{R}}{TN} E_\sigma \left\{ \left[ \sum_{t=1}^T (\boldsymbol{\sigma}'_t \mathbf{K}_t \boldsymbol{\sigma}_t)^{\frac{s^*}{2}} \right]^{\frac{1}{s^*}} \right\} \\ &= \frac{2\sqrt{R}}{TN} E_\sigma \{ \|\mathbf{u}\|_{s^*} \}\end{aligned}\tag{37}$$

□

### 7.3 Proof to Theorem 1

*Proof.* First note that  $\forall s_1 > s_2 \geq 1$ , we have that  $1 \leq s_1^* < s_2^*$ , which means  $\|\mathbf{u}\|_{s_1^*} \geq \|\mathbf{u}\|_{s_2^*}$ . Based on Equation (37), we immediately have  $\hat{R}(\mathcal{F}_{s_1}) \geq \hat{R}(\mathcal{F}_{s_2})$ . This gives the monotonicity of  $\hat{R}(\mathcal{F}_s)$  with respect to  $s$ . □

### 7.4 Proof to Theorem 2

*Proof.* Similar to the proof to Lemma 2, we write the ERC of  $\tilde{\mathcal{F}}$ :

$$\hat{R}(\tilde{\mathcal{F}}) = \frac{2}{TN} E_\sigma \left\{ \sup_{\boldsymbol{\alpha}_t \in \tilde{\mathcal{F}}} \sum_{t=1}^T \boldsymbol{\sigma}'_t \mathbf{K}_t \boldsymbol{\alpha}_t \right\}\tag{38}$$

Optimize with respect to  $\boldsymbol{\alpha}_t$  gives

$$\hat{R}(\tilde{\mathcal{F}}) = \frac{2\sqrt{R}}{TN} E_\sigma \left\{ \sum_{t=1}^T \sqrt{\boldsymbol{\sigma}'_t \mathbf{K}_t \boldsymbol{\sigma}_t} \right\}\tag{39}$$

Based on Lemma 2, we immediately obtain  $\hat{R}(\tilde{\mathcal{F}}) = \hat{R}(\mathcal{F}_{+\infty})$ . □

### 7.5 Proof to Theorem 3

*Proof.* According to Equation (37) and Jensen's Inequality, we have

$$\begin{aligned}\hat{R}(\mathcal{F}_s) &\leq \frac{2\sqrt{R}}{TN} \left( \sum_{t=1}^T E_\sigma \{ (\boldsymbol{\sigma}'_t \mathbf{K}_t \boldsymbol{\sigma}_t)^{\frac{s^*}{2}} \} \right)^{\frac{1}{s^*}} \\ &= \frac{2\sqrt{R}}{TN} \left( \sum_{t=1}^T E_\sigma \left\{ \left\| \sum_{i=1}^N \sigma_t^i \phi(\mathbf{x}_t^i) \right\|^{s^*} \right\} \right)^{\frac{1}{s^*}}\end{aligned}\tag{40}$$

Based on Lemma 5, we have that

$$\begin{aligned}\hat{R}(\mathcal{F}_s) &\leq \frac{2\sqrt{R}}{TN} \left( \sum_{t=1}^T (s^* \text{tr}(\mathbf{K}_t))^{\frac{s^*}{2}} \right)^{\frac{1}{s^*}} \\ &= \frac{2}{TN} \sqrt{R s^* \|\text{tr}(\mathbf{K}_t)_{t=1}^T\|_{\frac{s^*}{2}}}\end{aligned}\tag{41}$$

where  $\|\text{tr}(\mathbf{K}_t)_{t=1}^T\|_{\frac{s^*}{2}}$  denotes the  $l_{\frac{s^*}{2}}$ -norm of vector  $[\text{tr}(\mathbf{K}_1), \dots, \text{tr}(\mathbf{K}_T)]'$ . Since we assumed that  $k(\mathbf{x}, \mathbf{x}) \leq 1, \forall \mathbf{x}$ , we have

$$\begin{aligned}\hat{R}(\mathcal{F}_s) &\leq \frac{2}{TN} \sqrt{R s^* \left( \sum_{t=1}^T N \frac{s^*}{2} \right)^{\frac{2}{s^*}}} \\ &= \frac{2}{T\sqrt{N}} \sqrt{R T \frac{2}{s^*} s^*}\end{aligned}\tag{42}$$

Note that this bound can be further improved for the interval  $s \in [1, \rho^*]$ . To make this improvement, we first prove that  $\hat{R}(\mathcal{F}_s) \leq T^{\frac{1}{s'} - \frac{1}{s}} \hat{R}(\mathcal{F}_{s'})$  for any  $s' \geq s \geq 1$ .

$$\begin{aligned}
\hat{R}(\mathcal{F}_s) &= \frac{2}{TN} E_\sigma \left\{ \sup_{\lambda \geq \mathbf{0}, \|\lambda\|_s \leq 1} \sum_{t=1}^T \lambda_t \sqrt{\sigma'_t \mathbf{K}_t \sigma_t R} \right\} \\
&\leq \frac{2}{TN} E_\sigma \left\{ \sup_{\lambda \geq \mathbf{0}, \|\lambda\|_{s'} \leq T^{\frac{1}{s'} - \frac{1}{s}}} \sum_{t=1}^T \lambda_t \sqrt{\sigma'_t \mathbf{K}_t \sigma_t R} \right\} \\
&= \frac{2}{TN} E_\sigma \left\{ \sup_{\lambda \geq \mathbf{0}, \|\lambda\|_{s'} \leq 1} \sum_{t=1}^T T^{\frac{1}{s'} - \frac{1}{s}} \lambda_t \sqrt{\sigma'_t \mathbf{K}_t \sigma_t R} \right\} \\
&= T^{\frac{1}{s'} - \frac{1}{s}} \hat{R}(\mathcal{F}_{s'})
\end{aligned} \tag{43}$$

Based on this conclusion, we have that  $\forall s \in [1, \rho^*]$ ,

$$\begin{aligned}
\hat{R}(\mathcal{F}_s) &\leq T^{\frac{1}{\rho^*} - \frac{1}{s}} \hat{R}(\mathcal{F}_{\rho^*}) \\
&= T^{\frac{1}{\rho^*} - \frac{1}{s}} \frac{2}{TN} \sqrt{2eRN \log T} \\
&= T^{\frac{1}{\rho^*} - 1 + 1 - \frac{1}{s}} \frac{2}{TN} \sqrt{2eRN \log T} \\
&= \frac{T^{\frac{1}{s}}}{T^{\frac{1}{\rho^*}}} \frac{2}{TN} \sqrt{2eRN \log T} \\
&= \frac{T^{\frac{1}{s}}}{\sqrt{e}} \frac{2}{TN} \sqrt{2eRN \log T} \\
&= \frac{2}{T\sqrt{N}} \sqrt{RT^{\frac{2}{s}} \rho}
\end{aligned} \tag{44}$$

Note that this is always less than  $\frac{2}{T\sqrt{N}} \sqrt{RT^{\frac{2}{s^*}} s^*}$  that is given in (42);  $\rho^*$  is the global minimizer of the expression in (42) as a function of  $s$ . In summary, we have  $\hat{R}(\mathcal{F}_s) \leq \frac{2}{T\sqrt{N}} \sqrt{RT^{\frac{2}{s^*}} \rho}$  when  $s \in [1, \rho^*]$ , and  $\hat{R}(\mathcal{F}_s) \leq \frac{2}{T\sqrt{N}} \sqrt{RT^{\frac{2}{s^*}} s^*}$  when  $s > \rho^*$ .  $\square$

## 7.6 Proof to Lemma 3

*Proof.* Define  $\mathbf{K}_t \triangleq \sum_{m=1}^M \theta_m \mathbf{K}_t^m$ ,  $\forall t$ , then we can write

$$\hat{R}(\mathcal{F}_{s,r}) = \frac{2}{TN} E_\sigma \left\{ \sup_{\alpha_t \in \mathcal{F}_{s,r}} \sum_{t=1}^T \lambda_t \sigma'_t \mathbf{K}_t \alpha_t \right\} \tag{45}$$

where  $\mathcal{F}_s = \{\alpha_t \mid \alpha'_t \mathbf{K}_t \alpha_t \leq \lambda_t^2 R, \forall t; \lambda \in \Omega_s(\lambda); \theta \in \Omega_r(\theta)\}$ . Then using the similar proof of Lemma 2, we have that

$$\begin{aligned}
\hat{R}(\mathcal{F}_{s,r}) &= \frac{2\sqrt{R}}{TN} E_\sigma \left\{ \sup_{\theta \in \Omega_r(\theta)} \left[ \sum_{t=1}^T (\sigma'_t \mathbf{K}_t \sigma_t)^{\frac{s^*}{2}} \right]^{\frac{1}{s^*}} \right\} \\
&= \frac{2\sqrt{R}}{TN} E_\sigma \left\{ \sup_{\theta \in \Omega_r(\theta)} \sum_{t=1}^T (\theta' \mathbf{u}_t)^{\frac{s^*}{2}} \right\}^{\frac{1}{s^*}}
\end{aligned} \tag{46}$$

This gives the first equation in Equation (13). To prove the second equation, we simply optimize (46) with respect to  $\theta$ , which directly gives the result.  $\square$



## 7.7 Proof to Theorem 4

*Proof.* Consider Equation (13) and let  $g(\boldsymbol{\lambda}) \triangleq \sup_{\boldsymbol{\alpha} \in \Omega(\boldsymbol{\lambda})} \|\mathbf{v}\|_{r^*}$ . Then

$$\hat{R}(\mathcal{F}_{s,r}) = \frac{2}{TN} E_{\sigma} \left\{ \sup_{\boldsymbol{\lambda} \in \Omega_s(\boldsymbol{\lambda})} g(\boldsymbol{\lambda}) \right\} \quad (47)$$

Note that  $\forall 1 \leq s_1 < s_2$ , we have the relation  $\Omega_{s_1}(\boldsymbol{\lambda}) \subseteq \Omega_{s_2}(\boldsymbol{\lambda})$ . Therefore, let  $\hat{\boldsymbol{\lambda}}_1, \hat{\boldsymbol{\lambda}}_2$  be the solution of problems  $\sup_{\boldsymbol{\lambda} \in \Omega_{s_1}(\boldsymbol{\lambda})} g(\boldsymbol{\lambda})$  and  $\sup_{\boldsymbol{\lambda} \in \Omega_{s_2}(\boldsymbol{\lambda})} g(\boldsymbol{\lambda})$  correspondingly, we must have  $g(\hat{\boldsymbol{\lambda}}_1) \leq g(\hat{\boldsymbol{\lambda}}_2)$ . This directly implies  $\hat{R}(\mathcal{F}_{s_1,r}) \leq \hat{R}(\mathcal{F}_{s_2,r})$ .  $\square$

## 7.8 Proof to Theorem 5

*Proof.* Define  $\mathbf{K}_t \triangleq \sum_{m=1}^M \theta_m \mathbf{K}_t^m, \forall t$ , then

$$\hat{R}(\tilde{\mathcal{F}}_r) = \frac{2}{TN} E_{\sigma} \left\{ \sup_{\boldsymbol{\alpha}_t \in \tilde{\mathcal{F}}} \sum_{t=1}^T \boldsymbol{\sigma}'_t \mathbf{K}_t \boldsymbol{\alpha}_t \right\} \quad (48)$$

Fix  $\boldsymbol{\theta}$  and optimize with respect to  $\boldsymbol{\alpha}_t$  gives

$$\hat{R}(\tilde{\mathcal{F}}_r) = \frac{2}{TN} \sqrt{R} E_{\sigma} \left\{ \sup_{\boldsymbol{\theta} \in \Omega_r(\boldsymbol{\theta})} \sum_{t=1}^T \sqrt{\boldsymbol{\theta}' \mathbf{u}_t} \right\} \quad (49)$$

Based on Equation (13), we immediately obtain  $\hat{R}(\tilde{\mathcal{F}}_r) = \hat{R}(\mathcal{F}_{+\infty,r})$ .  $\square$

## 7.9 Proof to Theorem 6

*Proof.* Based on Equation (13) and Hölder's Inequality, let  $c \triangleq \max\{0, \frac{1}{r^*} - \frac{2}{s^*}\}$  we have that

$$\begin{aligned} \hat{R}(\mathcal{F}_{s,r}) &\leq \frac{2}{TN} \sqrt{R} E_{\sigma} \left\{ \sup_{\boldsymbol{\theta} \in \Omega_r(\boldsymbol{\theta})} \sum_{t=1}^T (\|\boldsymbol{\theta}\|_r \|\mathbf{u}_t\|_{r^*})^{\frac{s^*}{2}} \right\}^{\frac{1}{s^*}} \\ &= \frac{2}{TN} \sqrt{R} E_{\sigma} \left\{ \sum_{t=1}^T \|\mathbf{u}_t\|_{r^*}^{\frac{s^*}{2}} \right\}^{\frac{1}{s^*}} \\ &\leq \frac{2}{TN} \sqrt{RM^c} E_{\sigma} \left\{ \sum_{t=1}^T \|\mathbf{u}_t\|_{\frac{s^*}{2}}^{\frac{s^*}{2}} \right\}^{\frac{1}{s^*}} \end{aligned} \quad (50)$$

Applying Jensen's Inequality, we have that

$$\begin{aligned} \hat{R}(\mathcal{F}_{s,r}) &\leq \frac{2}{TN} \sqrt{RM^c} \left( \sum_{t,m=1}^{T,M} E_{\sigma} \left\{ (u_t^m)^{\frac{s^*}{2}} \right\} \right)^{\frac{1}{s^*}} \\ &= \frac{2}{TN} \sqrt{RM^c} \left( \sum_{t,m=1}^{T,M} E_{\sigma} \left\| \sum_{i=1}^N \sigma_t^i \phi_m(\mathbf{x}_t^i) \right\|^{s^*} \right)^{\frac{1}{s^*}} \end{aligned} \quad (51)$$

Using Lemma 5, we have that

$$\hat{R}(\mathcal{F}_{s,r}) \leq \frac{2}{TN} \sqrt{RM^c s^*} \left( \sum_{t,m=1}^{T,M} (\text{tr}(\mathbf{K}_t^m))^{\frac{s^*}{2}} \right)^{\frac{1}{s^*}} \quad (52)$$

Since we assume that  $k_m(\mathbf{x}, \mathbf{x}) \leq 1, \forall m, \mathbf{x}$ , we have that

$$\hat{R}(\mathcal{F}_{s,r}) \leq \frac{2}{T\sqrt{N}} \sqrt{R s^* T^{\frac{2}{s^*}} M^{\max\{\frac{1}{r^*}, \frac{2}{s^*}\}}} \quad (53)$$

$\square$

## 7.10 Proof to Corollary 1

*Proof.* First, by following the same proof of  $\hat{R}(\mathcal{F}_s) \leq T^{\frac{1}{s'} - \frac{1}{s}} \hat{R}(\mathcal{F}_{s'})$  for any  $s' \geq s \geq 1$ , we can directly obtain the conclusion that  $\hat{R}(\mathcal{F}_{s,r}) \leq T^{\frac{1}{s'} - \frac{1}{s}} \hat{R}(\mathcal{F}_{s',r})$  for any  $s' \geq s \geq 1$ .

When  $r^* \leq \log T$  and  $s \in [1, \rho^*]$ , where  $\rho = 2 \log T$ , we have that

$$\begin{aligned} \hat{R}(\mathcal{F}_{s,r}) &\leq T^{\frac{1}{\rho^*} - \frac{1}{s}} \hat{R}(\mathcal{F}_{\rho^*,r}) \\ &= \frac{2T^{\frac{1}{\rho^*}}}{T\sqrt{Ne}} \sqrt{2eRM^{\frac{1}{\rho^*}} \log T} \\ &= \frac{2}{T\sqrt{N}} \sqrt{RT^{\frac{2}{\rho^*}} \rho M^{\frac{1}{\rho^*}}} \end{aligned} \quad (54)$$

When  $s > \rho^*$ , obviously, we have  $\hat{R}(\mathcal{F}_{s,r}) \leq \frac{2}{T\sqrt{N}} \sqrt{RT^{\frac{2}{s^*}} s^* M^{\frac{1}{s^*}}}$

Similarly, for  $r^* \geq \log MT$  and  $s \in [1, \rho^*]$ , where  $\rho = 2 \log MT$ , we have that

$$\begin{aligned} \hat{R}(\mathcal{F}_{s,r}) &\leq T^{\frac{1}{\rho^*} - \frac{1}{s}} \hat{R}(\mathcal{F}_{\rho^*,r}) \\ &= \frac{T^{\frac{1}{\rho^*}}}{\sqrt{T^{\frac{1}{\log MT}}}} \frac{2}{T\sqrt{N}} \sqrt{2Re \log MT} \\ &= \frac{2}{T\sqrt{N}} \sqrt{2RT^{\frac{2}{s^*}} M^{\frac{1}{\log MT}} \log MT} \\ &= \frac{2}{T\sqrt{N}} \sqrt{RT^{\frac{2}{s^*}} \rho M^{\frac{2}{\rho}}} \end{aligned} \quad (55)$$

When  $s > \rho^*$ , obviously, we have  $\hat{R}(\mathcal{F}_{s,r}) \leq \frac{2}{T\sqrt{N}} \sqrt{RT^{\frac{2}{s^*}} s^* M^{\frac{2}{s^*}}}$   $\square$

## 7.11 Proof to Theorem 7

*Proof.* We have already show that the ERC of  $\mathcal{F}_s$  is

$$\hat{R}(\mathcal{F}_s) = \frac{2}{TN} E_\sigma \left\{ \sup_{\alpha, \lambda} \sum_{t=1}^T \sigma'_t \mathbf{K}_t \alpha_t \right\} \quad (56)$$

It is not difficult to see that optimizing the following problem

$$\begin{aligned} &\sup_{\alpha, \lambda} \sum_{t=1}^T \sigma'_t \mathbf{K}_t \alpha_t \\ &s.t. \alpha'_t \mathbf{K}_t \alpha_t \leq \lambda_t^2 R \\ &\quad \|\lambda\|_s \leq 1 \end{aligned} \quad (57)$$

with respect to  $\alpha_t$  must achieves its optimum at the boundary, *i.e.*, the optimal  $\alpha_t$  must satisfy  $\alpha'_t \mathbf{K}_t \alpha_t = \lambda_t^2 R$ . Therefore, Problem (57) can be re-written as

$$\begin{aligned} &\sup_{\alpha, \lambda} \sum_{t=1}^T \sigma'_t \mathbf{K}_t \alpha_t \\ &s.t. \alpha'_t \mathbf{K}_t \alpha_t = \lambda_t^2 R \\ &\quad \|\lambda\|_s \leq 1 \end{aligned} \quad (58)$$

Substituting the first constraint into the second one directly leads to the result. The proof regarding to  $\mathcal{F}_{s,r}$  is similar, and therefore we omit it.  $\square$